Article

Specific Formation of Beads-on-a-Chain Structures on Giant DNA Using a Designed Polyamine Derivative

Ning Chen, Anatoly A. Zinchenko, Shizuaki Murata, and Kenichi Yoshikawa

J. Am. Chem. Soc., **2005**, 127 (31), 10910-10916• DOI: 10.1021/ja042509q • Publication Date (Web): 19 July 2005

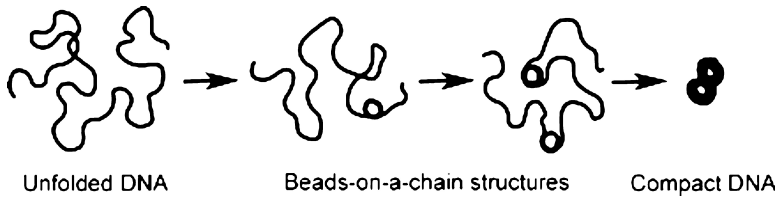

More About This Article

Additional resources and features associated with this article are available within the HTML version:

- Supporting Information
- Links to the 2 articles that cite this article, as of the time of this article download
- Access to high resolution figures
- Links to articles and content related to this article
- Copyright permission to reproduce figures and/or text from this article

View the Full Text HTML

J|A|C|S
ARTICLES
Published on Web 07/19/2005

Specific Formation of Beads-on-a-Chain Structures on Giant DNA Using a Designed Polyamine Derivative

Ning Chen,[†,‡] Anatoly A. Zinchenko,[‡] Shizuaki Murata,*[,†,§] and Kenichi Yoshikawa[‡,§]

Contribution from the Graduate School of Environmental Studies, Nagoya University, Chikusa, Nagoya 464-8601 Japan, Department of Physics, Kyoto University, Sakyo, Kyoto 608-8501, Japan, and CREST JST (Japan Science and Technology Agency)

Received December 14, 2004; E-mail: murata@urban.env.nagoya-u.ac.jp

Abstract: Fluorescence microscopy was used to study the folding transition of giant DNAs, T4 DNA (ca. 166 kbp), and λ DNA (ca. 48 kbp), which proceeds through intermediates with intramolecular segregation induced by pteridine−polyamine conjugates, i.e., 2-amino-6,7-dimethyl-4-(4,9,13-triazatridecylamino)pteridine and -4-(3-(aminopropyl)amino)pteridine. According to the results of DNA denaturation, UV and fluorescent spectroscopy, and transmission electron microscopic observations, it became clear that DNA folding induced by the polyamine derivative is not a continuous shrinking process but a combination of discontinuous processes.

Introduction

The DNA compaction process, induced by various condensing agents, has attracted significant interest not only due to its potential applicability for gene delivery techniques[1,2] but also to gain a better understanding of the mechanism of DNA packaging in living organisms.[3−5] It is already known that there exist large discrete differences between the densities of DNA macromolecular segments on the order of 10^4 between the compacted and elongated states.[6] Extensive studies on the folding transition of individual DNA chains in the presence of DNA condensing agents have revealed that the compaction process can proceed by two different scenarios; those are interchain segregation and intrachain segregation.[7] In the former scenario, where the compaction transition proceeds in an all-or-none manner at the level of individual chains,[8,9] individual DNA molecules in elongated coil and folded compact states coexist at a certain concentration of a condensing chemical. In the latter scenario, the folded and unfolded DNA conformations coexist along an individual DNA chain.[10−12] The appearance of this intrachain segregation on a DNA molecule is of potential significance in the context of modern postgenome investigations, because specific generation of partially unfolded genes (activation) in chromatin has been considered as an important mechanism controlling gene expression.[13,14]

It is known that most DNA compaction agents can compact DNA into toroidal condensates.[15] The initial DNA compaction stage is regarded to be spontaneous formation of a single loop along the DNA chain.[16] However, the formation of multiply segregated centers on the long DNA chains has not been hitherto investigated, because in the cases of commonly employed short DNA molecules, the formation of the multiply segregation centers could not occur. On the other hand, theoretical attempts have recently simulated the process of long (genetic size) semiflexible chain compaction through intramolecular segregated structures.[17−21] It was generally assumed that limitations in the size of the compacted unit on DNA might determine the probable morphology of partially collapsed DNA chains (that is a number of the segregated centers on the chain).[17] A general approach to producing the intramolecular segregated state of a DNA chain has not yet been established, although the generation of segregated structures has been described in several recent reports.[11,22,23] A noteworthy finding reported in our recent

† Nagoya University.
‡ Kyoto University.
§ CREST JST.

(1) *Self-Assembling Complexes for Gene Delivery*; Kabanov, A. V., Felgner, Ph. L., Seymour, L. W., Eds.; Wiley: Chichester, 1998.
(2) Luo, D.; Saltzman, W. *Nat. Biotechnol.* **2000**, *18*, 33−37.
(3) Frenkiel-Krispin, B.; Ben-Avraham, I.; Englander, J.; Shimoni, E.; Wolf, S. G.; Minsky, A. *Mol. Microbiol.* **2004**, *51*, 395−405.
(4) Levin-Zaidman, S.; Englander, J.; Shimoni, E.; Sharma, A. K.; Minton, K. W.; Minsky, A. *Science* **2003**, *299*, 254.
(5) Hud, N. V.; Allen, M. J.; Downing, K. H.; Lee, J.; Balhorn, R. *Biochem. Biophys. Res. Commun.* **1993**, 1347−1354.
(6) Bloomfield, V. A. *Curr. Opin. Struct. Biol.* **1996**, *6*, 334−341.
(7) Iwaki, T.; Yoshikawa, K. *Phys. Rev. E* **2003**, *68*, 031902.
(8) Lifshitz, I. M.; Grosberg, A. Y.; Khokhlov, A. R. *Rev. Mod. Phys.* **1978**, *50*, 683−713.
(9) Vasilevskaya, V. V.; Khokhlov, A. R.; Matsuzawa, Y.; Yoshikawa, K. *J. Chem. Phys.* **1995**, *102*, 6595−6602.
(10) Takagi, S.; Tsumoto, K.; Yoshikawa, K. *J. Chem. Phys.* **2001**, *114*, 6942−6949.
(11) Ueda, M.; Yoshikawa, K. *Phys. Rev. Lett.* **1996**, *77*, 2133−2136.
(12) Yoshikawa, K.; Yoshikawa, Y.; Koyama, Y.; Kanbe, T. *J. Am. Chem. Soc.* **1997**, *119*, 6473−6477.
(13) Mohd-Sarip, A.; Verrijzer, C. P. *Science* **2004**, *306*, 1484−1485.
(14) Gibbs, W. W. *Sci. Am.* **2003**, *12*, 80−85.
(15) Gosule, L. C.; Schellman, J. A. *Nature* **1976**, *259*, 333−335.
(16) Hud, N. V.; Downing, K. H.; Balhorn, R. *Proc. Natl. Acad. Sci. U.S.A.* **1995**, *92*, 3581−3585.
(17) Sakaue, T. *J. Chem. Phys.* **2004**, *120*, 6299−6305.
(18) Dobrynin, A. V.; Rubinstein, M.; Obukhov, S. P. *Macromolecules* **1996**, *29*, 2974−2979.
(19) Chodanowski, P.; Stoll, S. *J. Chem. Phys.* **1999**, *111*, 6069−6081.
(20) Lyulin, A. V.; Dunweg, B.; Borisov, O. V.; Darinskii, A. A. *Macromolecules* **1999**, *32*, 3264−3278.
(21) Micka, U.; Kremer, K. *Europhys. Lett.* **2000**, *49*, 189−195.
(22) Zinchenko, A. A.; Sergeyev, V. G.; Murata, S.; Yoshikawa, K. *J. Am. Chem. Soc.* **2003**, *125*, 4414−4415.
(23) Starodoubtsev, S. G.; Yoshikawa, K. *J. Phys. Chem.* **1996**, *100*, 19702−19705.

10.1021/ja042509q CCC: $30.25

paper[22] suggested that the suitable molecular design of DNA condensing chemicals can control morphology of the segregated DNA.

In this paper, we would like to describe the detailed scenario of the long DNA chain conformational transition from coil to globule states through conformational intermediates with intrachain segregation. This DNA transition was induced by the action of pteridine−polyamine conjugates, those are 2-amino-4-(3-aminopropyl)amino-6,7-dimethylpteridine (PT-4DAP) and 2-amino-4-(4,9,13-triazatridecyl)amino-6,7-dimethylpteridine (PT-4SPM), both of which were synthesized as analogues of naturally occurring oncopterin. Oncopterin was isolated from cancer (malignant lymphoma) patients and considered to be a potential marker for a cancer diagnosis.[24−26] The choice of such compaction agents was favored by their strong potential to create intrachain segregation on DNA.

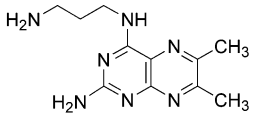

PT-4DAP

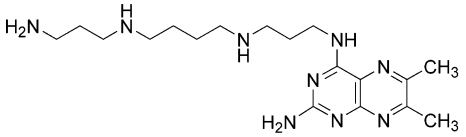

PT-4SPM

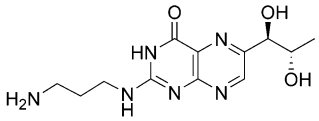

Oncopterin

Experimental Section

Materials. Bacteriophage T4 DNA (166 000 base pairs), λ DNA (48 500 base pairs), and calf thymus DNA (sheared, 200−500 base pairs) were purchased from Nippon Gene Co., Ltd., Takara Bio Inc., and R&D Systems, Inc., respectively. The fluorescent dye, 1,1′-[1,3-propanediylbis[(dimethyliminio)-3,1-propanediyl]]bis[4-[(3-methyl-2(3H)-benzox azolylidene) methyl]]quinolinium tetraiodide (YOYO-1, λ_{max} (ex) = 508 nm) was obtained from Molecular Probes, Inc.; 2-mercaptoethanol, 1,3-diaminopropane, and spermine were obtained from Wako Pure Chemical Industries Ltd., Tokyo Kasei Kogyo Co., Ltd., and Sigma-Aldrich Co., respectively. Purified water in Milli-Q grade is referred to as water in this study.

Preparation of PT-4DAP. A mixture of 2,6-diamino-5-nitroso-4-pentyloxypyrimidine[27] (5.0 g, 22 mmol) and 5% palladium carbon (3.5 g) in 200 mL of methanol was shaken under hydrogen atmospheric pressure at room temperature. The catalyst was removed by filtration, and the solvent was removed by evaporation. The resulting 2,5,6-triamino-4-pentyloxypyrimidine was dissolved in 200 mL of methanol. To this was added 2 g (23 mmol) of diacetyl, and the solution was stirred for 4 h at room temperature. The mixture was evaporated, and the residue was recrystallized from methanol. 4-Pentyloxy-6,7-dimethylpterin (1.7 g, 35%) was obtained as yellow crystals. Mp 143−145 °C. ^{1}H NMR (400 Hz, $CDCl_3$): δ/ppm = 0.90 (t, J = 7.1 Hz, 3H), 1.39 (m, 4H), 1.90 (m, 2H), 4.54 (t, J = 7.1 Hz, 3H), 5.27 (br s, 2H). ^{13}C NMR (100 Hz, $CDCl_3$): δ/ppm = 13.93, 22.36, 22.37, 23.51, 27.89, 28.15, 68.16, 121.16, 149.26, 155.87, 160.47, 160.79, 167.25.

A mixture of 0.42 g (1.59 mmol) of 4-pentyloxy-6,7-dimethylpterin and 0.87 g (7.69 mmol) of 1,3-diaminopropane was heated at 60 °C for 20 h. The mixture was filtered, and the precipitates were washed with diethyl ether (5 × 20 mL). The yellow powder (0.30 g) thus obtained was recrystallized from methanol. PT-4DAP (0.22 g, 56%) was obtained as yellow crystals. Mp: 196−198 °C. ^{1}H NMR (400 Hz, CD_3OD): δ/ppm = 1.84 (m, 2H), 2.57 (s, 3H), 2.58 (s, 3H), 2.72 (t, J = 6.6 Hz, 2H), 3.65 (t, J = 6.3 Hz, 2H). ^{13}C NMR (100 Hz, CD_3OD): δ/ppm = 21.79, 22.97, 32.93, 38.46, 39.33, 121.59, 148.06, 154.84, 160.40, 162.41, 164.00. Anal. calcd ($C_{11}H_{17}N_7$): N, 39.65; C, 53.42; H, 6.93%. Found: N, 39.0; C, 53.21; H, 6.79%.

Preparation of PT-4SPM. A mixture of 4-pentyloxy-6,7-dimethylpterin 0.42 g (1.61 mmol) and 0.81 g (4.00 mmol) of spermine was heated at 60 °C for 2 days under an argon atmosphere. The mixture was filtered, and the precipitates were washed with dry diethyl ether (5 × 20 mL). The resulting yellow powder was recrystallized from ethanol. PT-4SPM (0.30 g, 50%) was obtained as yellow crystals. Mp: 180 °C (dec). ^{1}H NMR (400 Hz, CD_3OD): δ/ppm = 1.53 (m, 4 H), 1.66 (m, 2 H), 1.88 (m, 2 H), 2.58 (m, 16 H), 3.63 (m, 2 H). ^{13}C NMR (100 Hz, CD_3OD): δ/ppm = 21.84, 23.01, 28.25, 29.95, 33.38, 33.39, 39.33, 40.63, 47.70, 48.26, 50.49, 50.56, 121.55, 147.91, 154.78, 160.28, 162.16, 163.97.

Preparation of Sample Solutions. Sample solutions for the fluorescent microscopy studies were prepared by sequential mixing of water (400 μL), a 0.1 M Tris−HCl buffer solution (50 μL, pH = 7.60 at 25 °C), 2-mercaptoethanol (20 μL), a 2 μM YOYO solution (10 μL), and a 10 μM T4 or λ DNA solution (10 μL) in the order they are listed. After 30 min, to the solution was added an aqueous solution of the pteridine−polyamine conjugate, and the sample was gently mixed. A 0.5 mL volume of final sample solution containing 0.01 mM Tris−HCl buffer, 4% (v/v) 2-mercaptoethanol, 0.2 μM DNA, 0.04 μM YOYO, and the appropriate amount of PT-4DAP or PT-4SPM was obtained. The mixture was kept for an additionally 30−60 min at room temperature until it was used for observation.

Hydrodynamic flow stretching of DNA molecules was performed as follows. A drop of the DNA sample solution prepared as described above was placed on a slide glass surface, and it was fixed by rapid pressing down on a free edge of a cover glass. Thus, the solution was spread between two cover glasses as a thin film.

The solution used for transmission electron microscopic observation was prepared by mixing 1 μM T4 DNA with 50 μM of PT-4SPM or 20 μM of spermine in 0.01 M Tris−HCl buffer solution. Uranyl acetate (1% in water) was employed for negative staining prior to transmission electronic microscopy (TEM) observations.

A solution of 5 $\times 10^{-5}$ M lambda DNA or calf thymus DNA in 1 mM NaCl solution containing a varying concentration of an appropriate condensing agent was used for the DNA denaturation experiments.

Observation of DNA Denaturation. UV absorbance values (A) in the wavelength range 220−310 nm of a 5 × 10^{-5} M DNA solution were reordered on a Jasco U-550 UV/VIS spectrophotometer with a Jasco ETC-505T temperature controller in a 1.0 × 1.0 × 5.0 cm^3 quartz cell with every 2−5 °C step. The degree of denaturation was calculated by the equation $(A - A_0)/(A_{max} - A_0)$, where A_0 and A_{max} are values of DNA absorption (260 nm) at room temperature and at the point of complete denaturation, respectively.

Fluorescent Microscopy (FM) and Instruments. FM observations were carried out at room temperature as follows. The samples were illuminated with a 365-nm UV light (high-pressure Hg lamp), and fluorescence images of DNA molecules were observed using a Zeiss Axiovert 135 TV microscope equipped with a 100× oil-immersed lens and recorded on a videotape through a Hamamatsu SIT TV camera. The populations of DNA molecules in unfolded, segregated, or compact

(24) Sugimoto, T.; Ogiwara, S.; Teradaira, R.; Fujita, K.; Nagtsu, T. *Biogenic Amines* **1992**, *9*, 77−82.
(25) Ogiwara, S.; Hidaka, H.; Sugimoto, T.; Teradaira, R.; Fujita, K.; Nagatsu, T. *J. Biochem.* **1993**, *113*, 1−3.
(26) Hibiya, M.; Teradaira, R.; Sugimoto, T.; Fujita, K.; Nagatsu, T. *J. Chormatogr., B* **1995**, *672*, 143−148.
(27) Pfleiderer, W.; Lohrmann, R. *Chem. Ber.* **1961**, *94*, 12−18.

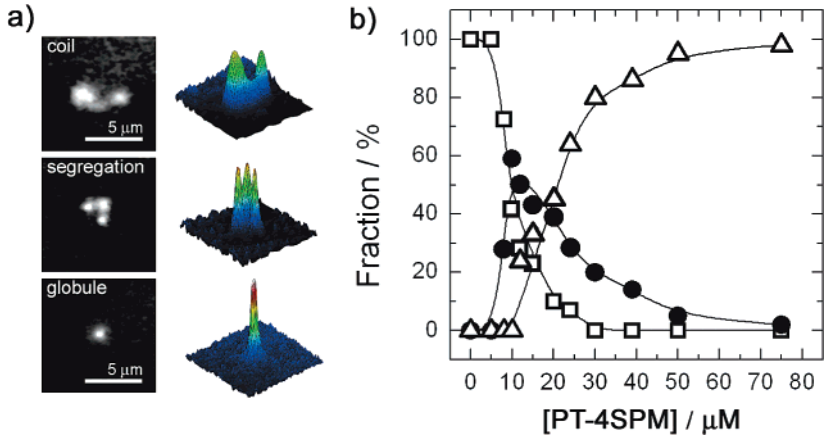

Figure 1. (a) Typical fluorescent images and corresponding fluorescent intensity profiles of T4 DNA individual molecule in coil, intrachain segregation, and globule states. (b) Relative populations of T4 DNA in coil (□), globule (△), and partially collapsed segregated states (●) at different concentrations of PT-4SPM. For every PT-4SPM concentration, at least 100 individual DNA chains were analyzed to calculate relative populations.

conformations in solution or on a glass surface were obtained by analysis of at least 100 DNA individual chains. Video records of fluorescent observations were analyzed with CosmosUI (v. 3.50) software.

UV, FM, CD, and NMR spectra were recorded on a Jasco U-550 UV/ VIS, a Jasco FP-6600, a Jasco J-790, and a JEOL A-400 spectrometers, respectively. TEM observations were carried out at room temperature on a JEM-1200EX microscope (JEOL) at an acceleration voltage of 100 kV using carbon-coated grids (mesh 300).

Results and Discussion

Single-Molecule Observation of DNA Compaction. The conformational states of T4 bacteriophage DNA (ca. 166 kbp, ca. 57 μm contour length[28]) stained with the fluorescent dye were monitored in highly diluted DNA solutions (0.2 μM) by the FM in the presence of different amounts of PT-4SPM. The conformations of the DNA chain in coil, globule, and intramolecular segregation states, in which both globule and coil parts coexisted on the same DNA molecule, were classified based on the shape as well as on the long axis length of the individual DNA fluorescent image (Figure 1a). For example, typical fluorescent profiles of T4 DNA in the globule and coil states appeared as a small-bright particle (long length axis: $L < 1$ μm) with rapid Brownian motion and a large-, hazy-, cloudlike image ($L = 3-5$ μm) with slower motion, respectively. In the segregated DNA molecule, both coil and globule states could be observed in the same DNA image. The distributions of these DNA conformational states as a function of PT-4SPM concentration are presented in Figure 1b. At low concentrations of PT-4SPM ($C < 7$ μM), all DNA molecules were recognized to be in the unfolded coil state. With increase in the condensing agent concentration ($C = 7-10$ μM), the amount of DNA in the coil conformation started to decrease, and the formation of DNA chains with the intrachain segregation was observed. At 10 μM of PT-4SPM, along with the decrease of the coil DNA fraction, completely collapsed DNA globules were observed. Finally ($C > 50$ μM), all DNA molecules were successively converted into globules. Figure 1b shows that the population of the segregated DNA passes through the maximum value, and at this point (PT-4SPM 10 μM), approximately 60% of DNA molecules in the mixture existed in the partially compacted form. Therefore, PT-4SPM primarily promoted the long DNA molecule compaction through intermediate states with the intrachain segregation.

The FM single-molecule observation in a bulk solution is useful for the analysis of distribution of individual DNA molecules in the various conformational states. However, it is rather difficult to obtain the detailed information about the morphology of individual DNA chains at different compaction stages due to DNA blurring effect[10] that enlarges the fluorescent image of DNA chain by ca. 0.3 μm in every dimension.

In comparison to uncertain FM images of DNA in the solution, clearer DNA images could be obtained by using the hydrodynamic flow stretching technique of DNA chain on a glass surface.[22] Typical examples of fluorescent images of coil, globule, and segregated T4 DNA molecules observed after the hydrodynamic flow stretching are shown in Figure 2. Appearance of the DNA in the globule state did not change after the stretching operation, whereas the full length of the DNA coil increased more than 10 times (from ca. 3.5 μm in the solution to ca. 57 μm on the glass surface) in the fully stretched form. Thence, such technique was useful for the specific elongation of the unfolded coil part. In the typical stretched DNA image with the intrachain segregation (Figure 2b), the compact globular part and the hazy stringlike coil part could be easily distinguished from each other. Since size of the compact part was too small to contribute significantly in the full measured length (L) of DNA, it was possible to estimate the proportion of the stretched coil part to the whole chain (i.e., the degree of DNA single chain compaction) as roughly L/L_{max}, which equals $L/57$ in the case of 57 μm T4 DNA. The stretching technique is generally useful for the analysis of the conformational transformation of other long DNA molecules (Supporting Information). For λ DNA, the phenomenon of intrachain segregation can be discussed in the same manner as for T4 DNA.

To gain good understanding of the DNA folding process through partially collapsed conformations, the morphology of the DNA segregation states was systematically characterized based on the full length of stretched DNA as well as the number of segregated centers on individual DNA chains at different concentrations of PT-4SPM. The dependence of the average length of segregated T4 DNA on the PT-4SPM concentration is given in Figure 3a. Here, with the increase of the PT-4SPM

(28) Yoshikawa, K.; Matsuzawa, Y.; Minagawa, K.; Doi, M.; Matsumoto, M. *Biochem. Biophys. Res. Commun.* **1992**, *188*, 1274−1279.

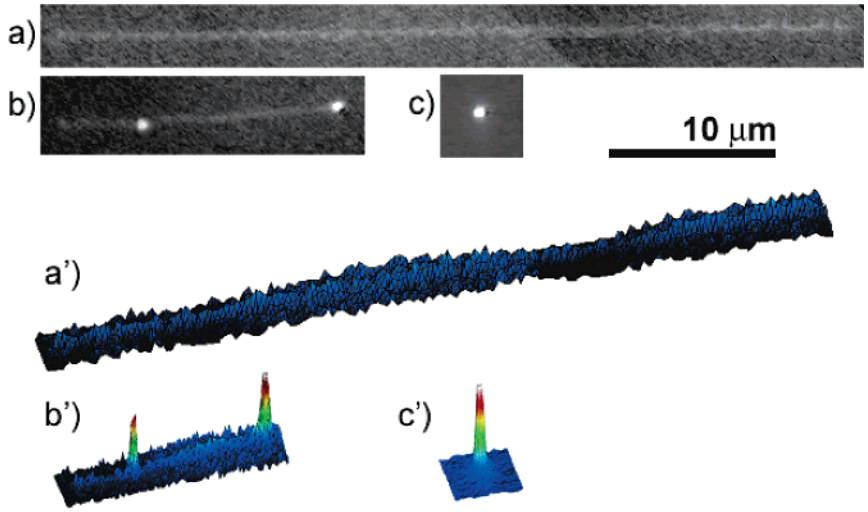

Figure 2. (a−c) Fluorescent images of stretched T4 DNA molecule in coil, intrachain segregation, and globule states, respectively. (a′−c′) The corresponding quasi-3D fluorescent intensity profiles.

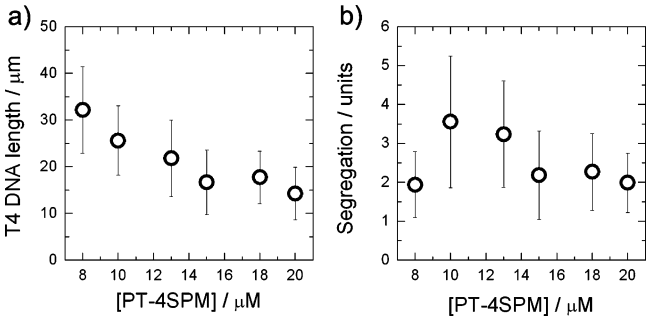

Figure 3. (a) Dependence of the average length of partially compact T4 DNA molecules at different concentrations of PT-4SPM. (b) Dependence of the average number of segregated units on partially compact T4 DNA molecules at different concentrations of PT-4SPM.

concentration ($C = 8-15\ \mu$M), the length of segregated DNA molecules decreases gradually, and it might be reasonable to consider the scenario that PT-4SPM promotes continuous compaction of individual T4 DNA chains from the coil to globule states through segregated intermediates with decreasing the length of the unfolded part. However, at higher PT-4SPM concentration ($C > 15\ \mu$M), there is no significant change of the DNA length until almost all (>90%) DNA molecules are converted to the globule state. Therefore, it seems that there exists a critical length (threshold) of the segregated DNA before the final collapse into globule.

The evolution of the average number of segregated units on the DNA chain with PT-4SPM concentration is shown in Figure 3b. At lower concentrations of the compacting agent ($C = 8\ \mu$M), the partial DNA compaction was recognized ($L = 32\ \mu$m, L/L_{max} 56%), and at this time the average number of compact nuclei per DNA chain was about 2. When the PT-4SPM concentration increased to 10 μM, the average number of segregated units increased about 2-fold. However, at higher concentrations of PT-4SPM ($C > 15\ \mu$M, ca. 70% compaction degree), the average morphology of the segregated DNA contained 2 segregated units. Such evolution of the number of segregated units suggests the existence of the competition between nucleation and merging of the segregation center on the long DNA chain. At the earlier stages of the DNA compaction (at lower concentrations of DNA condensing chemicals), the nucleation, that is, formation of new segregation centers on the DNA chain, dominates to induce the appearance of the multiple segregation on DNA. However, at the later stages of the DNA compaction, merging of segregated units becomes a prevalent process, and the average number of segregation units decreases. The decrease of the average length of segregated DNA chains and the similar evolution of segregation centers were also observed in the case of shorter λ DNA. The average number (1.4) of the segregation centers was smaller than in the case of T4 DNA, but the degree of compaction (L/L_{max}) was similar to the case of T4 DNA in the presence of the equal concentration of PT-4SPM.

Correlations between DNA length and the number of segregated units on T4 and λ DNAs at 20 μM concentration of PT-4SPM are given in parts a and b of Figure 4, respectively. At the fixed concentration of PT-4SPM, there is no significant variation in the relation between the length of unfolded DNA part and the number of segregated centers on individual molecules. The invariability of segregated DNA length was confirmed at other concentrations of PT-4SPM. The finding indicated that at middle to high PT-4SPM concentrations, where 30−60% of the DNA chain exists in the segregated form, the degree of DNA compaction is independent from the number of segregated units on the chain.

Chemical nature of the DNA condensing agent can influence strongly on the mechanism of the long DNA compaction. In relation to the results of PT-4SPM, we confirmed by using the similar FM analysis that spermine did not induce segregation structures during the DNA compaction. Instead, the compaction induced by spermine proceeded in an all-or-none fashion. On the other hand, in the T4 DNA compaction induced by less cationic PT-4DAP conjugate, although the transformation required higher concentration than in the case of PT-4SPM, the same tendency, namely, to produce intrachain segregation on the DNA chain was confirmed.

Physical and Spectroscopic Properties. As it was demonstrated by the FM observations, there was a diversity of intermediate DNA conformations with the intrachain segregation which was locating between DNA coil and globule states. It was expected that conformational stability of the intermediate differed from those of terminated states, since thermal behavior of DNA with different organization (liquid-crystalline, isotropic,

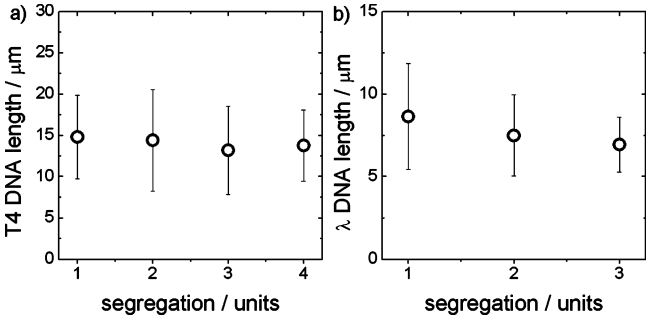

Figure 4. Dependence of the chain length of partially compact T4 DNA (a) and λ DNA (b) on the number of segregated centers in the presence of 20 μM PT-4SPM. The dependence for T4 DNA was built using experimental data for DNA length and number of segregated units of Figure 3.

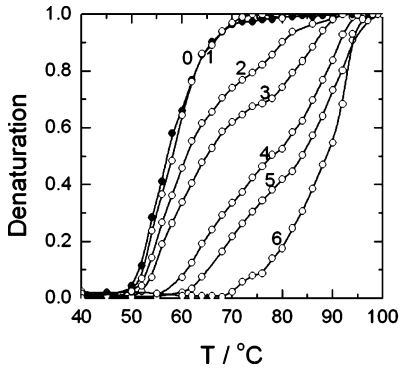

Figure 5. (a) Thermal denaturation curves of λ DNA (50 μM) in the presence of different amounts of PT-4SPM: (0, ●) without PT-4SPM, (1, ○) in the presence of 1 μM PT-4SPM, (2, ○) 2 μM, (3, ○) 3 μM, (4, ○) 5 μM, (5, ○) 7 μM, (6, ○) 10 μM.

gel) phases were reported to be different.[29,30] To monitor stability of morphology during the DNA compaction, we investigated thermal denaturation of DNA duplex in the presence of different concentrations of PT-4SPM. The denaturation curves of λ DNA in solutions containing different amounts of PT-4SPM are shown in Figure 5. With an increase of the PT-4SPM concentration, DNA melting (T_m) curve shifted toward higher temperatures. The result demonstrates a well-known cationic effect of DNA double-helix stabilization.[31] The DNA double helix is stabilized by the polycation because of reducing electrostatic repulsion in the strands and formation of bridge-bonding between the strands. Contrary to the melting curve of free DNA (the curve 0 in Figure 5), DNA melting curves in the presence of PT-4SPM (concentrations from 2 to 10 μM, curves 2−6) exhibited the characteristic two-step shape. With the increase of the PT-4SPM concentration, the ratio between the first and second steps on the T_m curves decreased, and the contribution of the second step increased. These results, in conjunction with the results obtained by the FM observations, suggest that the two-step DNA melting can be considered as a successive melting of DNA in the unfolded and compact conformations. The increase of the compaction agent concentration induced growth of the population of the partially compacted DNA in the sample solution, and therefore, the second T_m step that corresponded to the melting of the compacted part increased. By use of differentiated

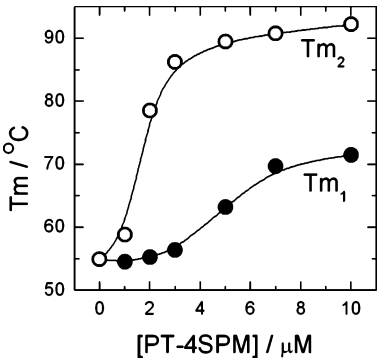

Figure 6. Dependences of first (T_{m_1}) (●) and second (T_{m_2}) (○) melting temperatures of λ DNA on the concentration of PT-4SPM. T_{m_1} and T_{m_2} were obtained using differentiated melting curves (Supporting Information) as the temperatures of first and second maximums, respectively.

melting curves, one can estimate melting temperatures T_{m_1} and T_{m_2} as the characteristic temperatures of the first and second melting steps, respectively. Thence, T_{m_1} and T_{m_2} values reflected stabilities of the DNA double strand in the unfolded conformation and in the compact state (segregated center), respectively. The dependences of T_{m_1} and T_{m_2} on PT-4SPM concentration are shown in Figure 6. Both T_{m_1} and T_{m_2} values increased with the concentration of PT-4SPM in the DNA solution, and the result indicated that stabilities of unfolded and compact states increased depending on the PT-4SPM concentration. The increase of the T_{m_2} value was large (>30 °C), and the fact suggested that the evolution of the segregated DNA morphology was accompanied with the increase of stability of the segregated centers.

The two-step DNA denaturation is not entirely a new finding, and indeed, a few examples have been discussed in the past literature.[32−34] Short DNA melting profiles in the presence of polycation were reported to have two clear steps.[34] It has been well understood that each melting step corresponded to successive melting of free DNA and a DNA complex with polycation. The first and second melting temperatures (T_{m_1} and T_{m_2}) were constant and independent from the concentration of polycation in the case of the short DNA−polycation complex. Contrary, the two-step melting of giant DNA induced by the pteridine−polyamine conjugate is of conceptually different origin. The T_{m_1} and T_{m_2} temperatures (Figure 6) increase considerably with the increase of the concentration of condensing agents, and the significant elevation of the T_{m_2} value indicates an increase of the stability of segregation center with higher DNA compaction degree. The melting curve of the long DNA chain supports the DNA compaction scenario via various segregated morphologies revealed by fluorescent microscopy. It also becomes obvious that stability of compact part in segregated DNA increases when it grows in size.

Here, we would like to discuss limitations for the occurrence of the two-step melting based on the DNA chain length. A thermal denaturation curve of short DNA fragments (sheared calf thymus DNA, 0.2−0.5 kbp) in the presence of 2 μM PT-4SPM is given in Figure 7 together with the T_m curve of λ DNA under the same conditions. Contrary to the case of longer λ

(29) Grasso, D.; Fasone, S.; La Rosa, C.; Silyanov, V. *Liq. Cryst.* **1991**, *9*, 299−305.
(30) Grasso, D.; Campisi, R. G.; La Rosa, C. *Thermochim. Acta* **1992**, *199* (1), 239−246
(31) Mahler, H. R.; Mehrotra, B. D. *Biochim. Biophys. Acta* **1963**, *68*, 211−233.
(32) Thomas, T. J.; Kulkarni, G. D.; Greenfield, N. J.; Shirahata, A.; Thomas, T. *Biochem. J.* **1996**, *319*, 591−599.
(33) Antony, T.; Thomas, T.; Shirahata, A.; Tomas, T. J. *Biochemistry* **1999**, *38*, 10775−10784.
(34) Shindler, T.; Nordmeier, E. *Polymer* **1999**, *40*, 7019−7027.

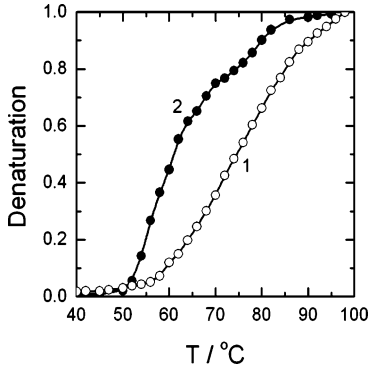

Figure 7. Thermal denaturation curves of long λ DNA (2, ●) and sheared calf thymus DNA (1, ○) in the presence of 2 μM of PT-4SPM.

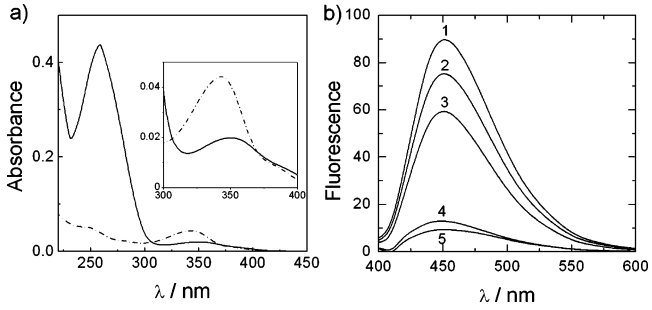

Figure 8. (a) UV spectra of 5 μM PT-4SPM (dash−dot line) and 5 μM PT-4SPM with 50 μM λ DNA (solid line). (b) Fluorescence spectra (λ_{ex} = 358 nm) of 50 nM PT-4SPM in 1 mM NaCl solution (1), and in the presence of λ DNA with concentrations of 0.1 nM (2), 1 nM (3), 10 nM (4), and 100 nM (5), respectively.

DNA, the denaturation curve of short DNA is a one-step profile, while it should appear as the two-step figure described in pervious papers. Thence, it is clear that the mechanism of PT-4SPM interaction with DNA duplex is conceptually different from those of usual polycationic condensing agents which afforded short DNA two-step melting. To understand the differences between the long and short DNA melting processes induced by PT-4SPM, it should be noted that the single-molecular DNA compaction is a specific phenomenon attributed only to DNA chains longer than about 10 kbp. Chain stiffness of DNA double strand does not allow short DNA fragments to a create a loop, which is one of most basic structures in the intrachain folding, and in such case neither DNA single-molecular compaction nor DNA intrachain segregation can be achieved.

Changes of UV and fluorescent spectra of PT-4SPM in the presence of DNA are shown in parts a and b of Figure 8, respectively. When λ DNA was added to a solution of PT-4SPM, a significant decrease of UV absorption in the range of 300−400 nm was found together with a red shift, see Figure 8a. Such UV shift is assigned as one of typical evidences of intercalation of the heterocyclic chromophore into DNA double strand.[35] Strong fluorescence (λ_{max} (em) = 451 nm) of PT-4SPM, was observed to be quenched effectively even in the presence of a small amount (1/500) of DNA (Figure 8b). The spectroscopic observations indicated the occurrence of a strong interaction as well as an energy transfer process between two heteroaromatic moieties of the pteridine−polyamine conjugate and DNA.

It is reasonable to assume that the electron-withdrawing pteridine part reduces electron density of binding nitrogen on it, and therefore, overall basicity of the PT-4SPM in a solution might reduce in comparison to spermine. Indeed, observed pK_a value (5.48 for PT-4SPM) suggests that one of four basic amino groups belonging to spermine is lost in PT-4SPM and that the polyamine part of PT-4SPM works as a +3 (not +4) charged ammonium ion when it interacts with DNA polyphosphate.[36] According to this assumption, PT-4SPM seems to afford weaker charge neutralizing interaction to DNA than spermine does. However, the strong duplex-interacting character of the pteridine part could carry the condensing agent specifically into a neighboring location of the DNA double helix, and this is one of reasons why the less charged condensing agent works well. Although pteridine and polyamine parts of the conjugate can operate individually on different parts of the DNA chain, the both parts concertedly achieve the DNA condensation.

A transmission electron microscope is a useful technique to gain insight into nanoscale morphologies of the DNA condensates. Parts a and b of Figure 9 show typical T4 DNA images in compact state obtained by adding 50 μM of PT-4SPM. All DNA condensates were indicating a clear tendency to form toroidal structures, which are typical for multication-inducing long DNA compacted states. However, in comparison with the structure (Figure 9c) of the typical single toroid created by spermine, PT-4SPM afforded DNA condensates consisting of a conglomerate of several small toroids. Here, it becomes clear that the formation of several small segregation centers (toroids) occurred prior to the complete collapse. It is known that the toroidal morphology of DNA consists of a highly organized hexagonal close-packed lattice;[37] therefore reorganization of already created small toroids into a single large toroid is considered to be difficult. The DNA chain length is the particularly important factor which is responsible for the appearance of multitoroid condensates because of stability limitation in larger DNA toroids. Previous reports clearly demonstrated that, in cases of short DNA molecules (with several kbp), the final toroidal condensate incorporated several DNA chains to increase thermodynamic stability of the compact phase.[38] A toroid structure of long DNA usually consists of only one DNA molecule. In contrast, the formation of multiply segregated intermediates under the specific conditions, as demonstrated by the example of PT-4SPM, would give the condensate of several toroids as the final DNA condensate.

By consideration of all the findings together, we would like to propose the following scenario for the DNA compaction induced by pteridine−polyamine conjugates. As revealed by the fluorescence study, even at very high dilution, PT-4SPM can interact with the DNA strand, but the DNA chain compaction does not occur due to the insufficient magnitude of charge neutralization. Once the amount of binding PT-4SPM on the DNA chain exceeds a threshold value, sufficient charge

(35) Reynisson, J.; Schuster, G. B.; Howerton, S. B.; Williams, L. D.; Barnett, R. N.; Cleveland, C. L.; Landman, U.; Harrit, N.; Chaires, J. B. *J. Am. Chem. Soc.* **2003**, *125*, 2072−2083.

(36) The relation of pk_a values with cationic characters of the pteridine−polyamine conjugates is discussed in the reference: Chen, N.; Murata, S.; Yoshikawa, K. *Chem.−Eur. J.*, in press.

(37) Hud, N. V.; Downing, K. H. *Proc. Natl. Acad. Sci. U.S.A.* **2001**, *98*, 14925−14930.

(38) Conwell, C. C.; Vilfan, I. D.; Hud, N. V. *Proc. Natl. Acad. Sci. U.S.A.* **2003**, *100*, 9296−9301.

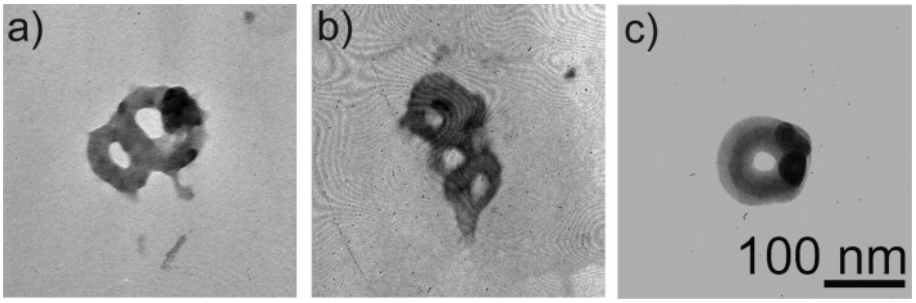

Figure 9. (a−b) Typical electron micrographs of T4 DNA (1 μM) collapsed by PT-4SPM (50 μM). (c) Typical electron micrograph of single T4 DNA molecule collapsed by spermine (20 μM).

neutralization creates the partial DNA chain folding, which affords several seeds of segregation. With an increase in the concentration of PT-4SPM in the solution, the segregated units grow up in size. Finally, they are assembled into one fully compacted conglomerate when the binding amount of PT-4SPM exceeds a critical value.

In conclusion, we successfully produced a sufficient amount of stable DNA molecules in intramolecular segregated states using a precisely designed pteridine−polyamine conjugate. In terms of the partially folded DNA intermediates, the DNA-compacting mechanism via the intramolecular segregation was found not to be a fully continuous process but to be a combination of discontinuous processes.

Acknowledgment. We thank Dr. Damien Baigl (Department of Physics, Kyoto University) for the kind help to carry out TEM observations. N.C. is grateful to NGK Insulators, Ltd., for the scholarship No. 04-10.

Supporting Information Available: Additional fluorescent microscopy images of stretched T4 and λ DNAs, figures of distributions of lengths and numbers of segregation centers in segregated T4 and λ DNAs, a figure of correlations between stretched T4 DNA average length and the number of segregation centers, and figures of differentiated DNA melting curves used to determine T_{m_1} and T_{m_2} temperatures. This material is available free of charge via the Internet at http://pubs.acs.org.

JA042509Q